HHS Public Access

Author manuscript

J Cutan Pathol. Author manuscript; available in PMC 2017 July 18.

Published in final edited form as:

J Cutan Pathol. 2016 June ; 43(6): 505–515. doi:10.1111/cup.12708.

Reflectance confocal microscopy features of mycosis fungoides and Sézary syndrome: correlation with histopathologic and T-cell receptor rearrangement studies

Silvia E. Mancebo[1], **Miguel Cordova**[1], **Patricia L. Myskowski**[1,2], **Eileen S. Flores**[1], **Klaus Busam**[3], **Sarah I. Jawed**[1,2], **Anna Skripnik**[1], **Milind Rajadhyaksha**[1], and **Christiane Querfeld**[1,4]

[1]Department of Medicine, Dermatology Service, Memorial Sloan Kettering Cancer Center, New York, NY, USA

[2]Department of Dermatology, Weill Cornell Medical College, New York, NY, USA

[3]Department of Pathology, Memorial Sloan Kettering Cancer Center, New York, NY, USA

[4]Department of Pathology and Dermatology, City of Hope Comprehensive Cancer Center, Duarte, CA, USA

Abstract

Background—Mycosis fungoides/Sézary syndrome (MF/SS) often requires multiple skin biopsies for definitive diagnosis. *In vivo* reflectance confocal microscopy (RCM) visualizes high-resolution cellular detail of the skin. The objective of this study is to evaluate the morphologic features of MF/SS using RCM and to correlate RCM features with histopathology and T-cell receptor (TCR) gene rearrangement studies.

Methods—A cohort of patients with active/recurrent or suspicious MF/SS disease was prospectively recruited for RCM imaging and histopathologic/RCM images were evaluated. Statistical analyses were performed to identify unique RCM features and to correlate RCM features with histopathologic findings and TCR rearrangement studies.

Results—Eighty-three lesions were evaluated. Correlation between RCM and histopathology was moderate for all relatable features ($\kappa = 0.41$, $p<0.001$), almost perfect for intraepidermal atypical lymphocytes [prevalence and bias-adjusted kappa (PABAK) = 0.90], and fair for Pautrier collections ($\kappa = 0.32$, $p = 0.03$). Lesions with Pautrier collections identified by RCM were significantly more likely to show TCR clonality ($p = 0.04$) and diagnostic features of MF/SS on histopathology ($p = 0.03$).

Conclusions—Our study captures morphologic RCM criteria for a variety of skin lesions. Pautrier collections visualized by RCM are associated with improved histopathologic diagnosis and detection of TCR gene clonality. Although further studies are needed to validate the diagnostic implications of RCM for MF/SS, our study highlights the potential utility of RCM.

Christiane Querfeld, MD, PhD, Dermatology/Dermatopathology Service, City of Hope Comprehensive Cancer Center, 1500 E. Duarte Road, Duarte, CA 90015, USA, Tel: (626) 256 4673 ext. 89018, Fax: (626) 301 8956, cquerfeld@coh.org.

Keywords

mycosis fungoides; RCM

Mycosis fungoides (MF) and Sézary syndrome (SS) are the most common types of cutaneous T-cell lymphoma (CTCL) and are characterized by clonal expansion of T-helper memory cells in the skin.[1,2] Both entities and in particular early patch stage MF frequently pose a diagnostic challenge due to heterogeneous and often non-specific clinical and histopathologic presentations.[3] Patients commonly undergo multiple biopsies before a diagnosis can be rendered. Consequently, a diagnostic algorithm for early MF was proposed by Guitart et al.[4] that takes the various histopathologic findings into account. Characteristic diagnostic features of classic MF/SS are a papillary dermal band-like infiltrate with irregular and/or hyperchromatic nuclei, variable findings of inflammatory cells and epidermotropism with infrequently seen Pautrier collections. Unusual clinical variants, such as hyperpigmented, poikilodermatous or chronic pigmented purpuric types, can be equally challenging to diagnose. Often, a reliable distinction from post-inflammatory changes cannot be made and emphasizes the high index of suspicion and frequent follow ups for repeated biopsies.

In vivo reflectance confocal microscopy (RCM) is a noninvasive imaging technique that provides high-resolution cellular detail of the epidermis and superficial dermis. Previously, RCM has been identified as a potentially useful tool in the evaluation of cutaneous lesions of MF.[5–9] Exploratory studies have successfully identified select features of MF, including epidermal lymphocytes and Pautrier collections. However, these studies were limited by sample size, inconsistent and varied methodologies, and discordant findings. Furthermore, these studies did not assess a wide range of lesion morphologies.

The aim of this study is to (a) expand the findings from previous studies by evaluating the RCM features of MF/SS in a large sample containing skin lesions of diverse morphology, (b) correlate RCM features of MF/SS with histopathologic findings and (c) T-cell receptor (TCR) gene rearrangement studies. We hypothesize that RCM may prove valuable in identifying features of MF/SS that may be used to detect optimal skin biopsy sites and to assess disease activity or treatment response.

Materials and methods

Study design

This study was approved by the Institutional Review Board and adhered to the principles set forth in the Declaration of Helsinki. Participants were prospectively recruited from October 2012 to February 2014 from the cutaneous lymphoma clinic. Eligible participants included (a) recently diagnosed MF/SS patients with biopsy-proven active disease, (b) previously diagnosed MF/SS patients suspected of disease recurrence and (c) patients referred to cutaneous lymphoma clinic for evaluation of suspected MF/SS.

Eligible patients were subjected to RCM imaging after written informed consent was obtained. For previously diagnosed MF/SS patients with active disease, the imaging site was

selected based on clinical and anatomical proximity to the most recent skin biopsy site demonstrating features of MF/SS. For patients who presented with recurrent or suspected MF/SS, RCM imaging was performed at clinically identified sites followed by a skin biopsy of at least one site.

Demographics, clinical information, including clinical stage and duration of symptoms were recorded for all participants. Results for histopathologic and TCR molecular studies were also recorded when performed.

RCM imaging and evaluation

RCM images were obtained using a commercially available reflectance confocal laser-scanning microscope [Vivascope 1500, Caliber Imaging and Diagnostics (Caliber ID; formerly, Lucid, Inc.), Rochester, NY, USA]. This system operates with an 830 nm diode laser with maximum power of 35 mW at tissue level and a 30× water immersion objective lens of 0.9 numerical aperture. After acquiring a macroscopic image, the lens was attached to the skin *via* an adhesive ring to reduce motion artifact during imaging. Mineral oil (refractive index: 1.50) served as the medium between the adhesive window and the skin. Ultrasound gel (refractive index: 1.34) served as the medium between the adhesive window and the lens. Comprehensive details of this system have been previously reported.[10,11]

Single high-resolution *en-face* images, representing noninvasive optical sections oriented parallel to the skin surface, with a field of view of 500 × 500 μm were captured. Mosaics of 16 × 16 images were compiled allowing for a larger field of view of 8 × 8 mm (Vivablock software, Caliber ID, Rochester, NY, USA). Mosaics were obtained for each lesion at the level of the stratum corneum, stratum spinosum, dermoepidermal junction (DEJ) and papillary dermis. Imaging in depth, with a field of view of 500 × 500 μm was performed in the select areas for each lesion. Images were captured in 1.5 μm steps starting at the stratum corneum to a maximum depth of 150–200 μm. The resolution markedly decreased below that depth (Vivastack software, Caliber ID, Rochester, NY, USA).

RCM evaluation was conducted in two stages. First, a subset of cases with clear histopathologic features of MF/SS was assessed for the detection of previously defined RCM parameters.[5,7] RCM definitions were refined and updated. Novel RCM features of MF/SS skin lesions were identified and described based on visual analysis of individual images in the mosaics. In the second stage, novel and updated RCM definitions were applied to the entire collection of RCM images for the identification of features of MF/SS.

Histopathologic evaluation

Skin biopsies were evaluated for features of MF/SS by two dermatopathologists with expertise in CTCL (KB and CQ). All skin biopsies, except tumor lesions, were evaluated using a standardized grading system for the diagnosis of MF as previously reported.[4] This grading system assigns a total score based on the presence of major and minor criteria and stratifies lesions as (a) perivascular infiltrate (score: 0–2), (b) atypical lymphocytic infiltrate, cannot rule out MF (score: 3–4), (c) atypical lymphocytic infiltrate, suggestive of MF (score: 5–6) and (d) MF (score: 7+). Lesions with a total score below 3 were excluded from the study, because of non-specific histopathologic findings.

Statistical analysis

Absolute and relative frequencies for RCM features were calculated and stratified by lesion morphology. Comparisons were calculated using a proportion test. Overall agreement between RCM and histopathology for all relatable features was obtained by calculating Cohen's kappa. Prevalence and bias-adjusted kappa (PABAK) was calculated for select RCM features where null data were absent or prevalence of a given response was too high or low. Kappa and PABAK values range between 1 and 0 with a value of 1.0 indicating full agreement beyond chance and value of 0 indicating no agreement beyond chance. A $p < 0.05$ was considered significant for all statistical tests. Data management and statistical analyses were performed using Stata v13.0 (Stata Corporation, College Station, TX, USA).

Results

Clinical characteristics

Forty-three participants were screened with a total of 86 lesions visualized by RCM over a period of 16 months. Two participants and three lesions were excluded from the study because of non-specific MF/SS histopathologic findings (score < 3) or histopathologic findings that were not consistent with MF/SS disease (i.e. granuloma annulare, folliculitis). Forty-one patients comprised the final participant pool (Fig. 1). Of these, 19 participants were recently diagnosed MF/SS and had previously received a biopsy to confirm active disease. The remaining 22 participants presented with skin lesions suspicious for MF/SS disease or disease recurrence, and 29 skin biopsies were performed in areas that were evaluated by RCM.

The final participant pool was composed of 26 men and 15 women with median age of 54 years (range: 25–86 years). Their ethnicity was as followed: 26 Caucasian, 6 African-American, 7 Hispanic and 4 Asian/Pacific Islander. Thirty-four participants had early stage disease (stage IA–IIA), and seven had advanced stage disease (stage IIB-IVB).

Of the 83 lesions included in the study, 72 lesions corresponded to 36 patients with MF, 8 lesions to 3 patients with folliculotropic MF, and 3 lesions to 2 patients with SS. A total of 56 patch lesions received RCM imaging, including 36 erythematous patches, 19 hyperpigmented patches and 1 hypopigmented patch. In addition, 20 plaques, 3 papules, 1 tumor and 3 erythrodermic skin lesions were imaged (Fig. 2).

RCM findings

Table 1 provides a complete list of RCM parameters captured in our patient population along with detailed morphologic descriptions. Perivascular infiltrate, follicular lymphocytes, melanophages in dermis and adnexal mucinous deposition in the follicular epithelium were identified as novel RCM features because they have not been well characterized among MF/SS patients.

Table 2 highlights the absolute and relative frequencies for select RCM parameters collected on the 83 lesions. Among all lesion morphologies, the most frequently observed RCM features were epidermal lymphocytes and epidermal disarray/loss of demarcation of

keratinocytes (Fig. 3A,B). Of note, Pautrier collections were observed in over 50% of lesions imaged (Fig. 3C,D).

Patch MF

Patch lesions were characterized by focal exocytosis of lymphocytes and perivascular infiltration of the papillary dermis (Fig. 4A,B). Differences between patches of various morphologies (i.e. erythematous, hyperpigmented) were noted at the level of DEJ and papillary dermis. Hyperpigmented patches were more likely to display hyper-reflective dermal papillae rings, compared with erythematous patches, which showed hypo-reflectivity of dermal papillae rings ($p < 0.001$). Melanophages in the dermis ($p < 0.001$) and lymphocyte tagging at DEJ ($p = 0.003$) were more often observed in hyperpigmented patches. Erythematous patches were characterized by increased blood vessel dilation ($p = 0.001$) and fibrosis ($p = 0.01$) of the papillary dermis (Fig. 4C,D).

Plaque MF

Pautrier collections ($p = 0.002$) and epidermal dendritic processes ($p < 0.001$) were more typical in plaques, compared with patches (Fig. 3C,D). At the DEJ level, most plaques showed hypo-reflective dermal papillae rings ($p = 0.04$), with 45% of lesions showing features of DEJ infiltration by lymphocytes.

Tumor MF

Only one tumor lesion was imaged. This lesion showed numerous small Pautrier collections and focal exocytosis of large, brightly reflective lymphocytes. There was marked epidermal disarray throughout the lesion and stellate cells with dendritic processes were observed in the stratum spinosum (Fig. 5A,B). At the level of the DEJ, the structure and arrangement of dermal papillae rings appeared disrupted. There was limited visualization of structures below the DEJ.

Erythrodermic MF/SS

Erythroderma was characterized by the presence of lymphocytes in the epidermis, DEJ and dermis. Prominent blood vessel dilation was observed in the papillary dermis; and compared with patches and plaques, dermal lymphocytes were more likely to be observed ($p = 0.003$ and $p = 0.01$, respectively).

Folliculotropic MF

Lymphocytes were found surrounding and invading the follicular epithelium (Fig. 6A–C). One patient showed concurrent mucinous deposition of the hair follicle (Fig. 6D).

RCM and histopathology correlation

Table 3 summarizes the correlation of RCM and histopathologic findings for the 29 lesions that were biopsied after RCM evaluation. Overall, RCM and histopathology were found to have moderate correlation ($\kappa = 0.41$, $p < 0.001$) with highest correlation for epidermal lymphocytes (PABAK = 0.90) and detection of melanophages in the dermis ($\kappa = 0.58$, $p = 0.007$). Pautrier collections had fair agreement ($\kappa = 0.32$, $p = 0.03$), with Pautrier collections

more commonly visualized on RCM (76 vs. 59%). Lymphocytes in the DEJ (PABAK = 0.24) and perivascular infiltrate ($\kappa = 0.21$, $p = 0.05$) had fair agreement, while lymphocytes in the dermis, blood vessel dilation and perifollicular infiltrate showed only slight agreement ($\kappa = 0.16$, $p = 0.14$; $\kappa = 0.15$, $p = 0.14$; $\kappa = 0.14$, $p = 0.21$).

RCM correlation to histologic grading criteria

Of 29 biopsies performed, 28 were assessed with the previously mentioned grading scheme for the histologic evaluation of MF. RCM evaluation of these lesions revealed that Pautrier collections were predictive of lesions with higher histologic scores. Among lesions scoring 7 or higher (consistent with MF), 100% of lesions displayed Pautrier collections on RCM, compared to only 53% of lesions scoring 3–6 ($p = 0.03$).

RCM correlation to TCR gene rearrangement

Twenty-four of the 29 biopsies performed were analyzed for TCR gene rearrangement. Ten biopsies showed monoclonal rearrangement of the TCR-beta (TCR-β) or TCR-gamma (TCR-γ) genes. Eleven biopsies did not reveal a TCR clone and three biopsies failed the TCR studies. Of the 24 biopsies tested, 3 out of 10 erythematous patches, 1 out of 5 hyperpigmented patches, 4 out of 7 plaques and 2 out of 3 erythrodermic skin lesions showed monoclonality of the TCR-β or TCR-γ genes. All lesions with monoclonal TCR genes displayed Pautrier collections on RCM, compared with 64% of lesions with negative or failed clonality ($p = 0.04$).

Discussion

Our study reports the RCM features of MF/SS in the largest cohort of CTCL patients examined to date. In this study, we have verified and confirmed previously reported RCM features and have characterized novel features that may represent important histologic clues of clinically active disease. By systematically assessing a cohort of patients with diverse lesion morphologies, we identified the most commonly represented RCM features, which include epidermal disarray (88%), epidermal lymphocytes (86%), blood vessel dilation (79%) and hypo-reflective dermal rings (72%). Furthermore, our study provides evidence that lesions with Pautrier collections identified on RCM are more likely to show TCR clonality and to display diagnostic features of MF/SS on histopathology.

Previous studies evaluating the RCM features of CTCL have reported mixed findings. Agero et al. were the first to investigate the RCM features of MF. They imaged eight MF lesions and descriptively reported epidermal lymphocytes, hypo-reflective dermal rings and Pautrier collections as the most striking features of MF on RCM.[5] They also identified the presence of Pautrier collections, but only among plaque-stage lesions. Koller et al. evaluated the RCM features of 75 erythematosquamous skin lesions, including 10 MF lesions.[6] They descriptively reported findings of interface dermatitis (herein referred to as DEJ lymphocytes), epidermal lymphocytes and large pleomorphic lymphocytes in MF. These findings, along with dendritic cells, were considered specific for MF. Koller et al. also reported that epidermal disarray and Pautrier collections had limited diagnostic applicability as these features were observed in other dermatoses.[6] Li et al. reported the RCM features of

10 MF lesions. These investigators observed epidermal lymphocytes, DEJ lymphocytes and hypo-reflective dermal rings in all MF lesions; however, Pautrier collections were only observed in 20% (n = 2) of lesions.[8] The limited sample sizes and varied methodologies used by previous studies preclude direct comparisons. However, these studies suggest that MF is characterized by non-specific patterns on RCM, as shown by the most commonly reported features (i.e. epidermal/DEJ lymphocytes, epidermal disarray and hypo-reflective dermal rings). These findings are mostly in line with our results and indeed reflect the protean nature of CTCL lesions that is often observed on histopathology.

Among the RCM features reported in this study, hypo- and hyper-reflective dermal rings are interesting observations. Hypo-reflective dermal rings were observed in the majority of lesions, but not all lesions as previously reported. This RCM feature has been formerly attributed to the presence of less reflective lymphocytes invading and surrounding the basal layer of the epidermis causing a relative decrease in the number of melanocytes and basal cells, which are normally considered to be moderately to strongly reflective.[5] Interestingly, we observed that a group of our patients, in particular patients with darker skin and hyperpigmented patches displayed hyper-reflective dermal rings on RCM. The importance of this finding is twofold. First, it shows potential differences between lesions of varied morphology and color. Second, it demonstrates that even in hyperpigmented patches, in which disease activity is often clinically challenging to determine, we retained the ability to identify discrete lymphocytes in the DEJ – a feature that may be an important diagnostic clue.

Another interesting observation is the prevalence and diagnostic importance of Pautrier collections detected by RCM. In our study, Pautrier collections were observed in 53% of lesions, compared to only 20% of lesions in the study reported by Li et al. Furthermore, compared to the study by Agero et al., we visualized Pautrier collections among all lesion morphologies, not only plaque-stage lesions. A possible explanation for these discrepancies is our RCM imaging protocol, which used a smaller interval for vertical stacks (1.5 vs. 5 μm) therefore allowing greater visualization of the epidermis. Other explanations include differences in RCM hardware, patient factors and operator experience. The study by Koller et al. reports that Pautrier collections have limited diagnostic applicability because of low specificity. Our study directly challenges this notion. In fact, our study demonstrates that lesions displaying Pautrier collections on RCM were more likely to yield samples that were clonal in nature and were more likely to be histologically consistent with MF/SS. Given that current dermatologic practice utilizes histologic assessment and molecular studies for the diagnosis of MF/SS and that these tests are often limited by paucity of cellular infiltrates, the methods used in this study highlight the potential value of noninvasively screening clinical sites prior to performing a skin biopsy. By identifying Pautrier collections on RCM, it may be possible to select areas that show specific histologic features of MF/SS and will yield a significant population of atypical (i.e. clonal) lymphocytes.

On a final note, our study reports novel RCM features of MF/SS that have not been previously well characterized. Of the four features reported, follicular lymphocytes and adnexal mucinous deposition are exciting features that were identified in patients with folliculotropic MF. These RCM features displayed invasion of the hair follicles with

lymphocytes and deposition of amorphous material within the hair epithelium. As folliculotropic MF has a worse overall prognosis, recognition of this disease subset is important for optimal management decisions.

Our study was limited by the two main factors. First, the current state of RCM technology limits visualization of structures beyond 200 μm in depth. In our study, vertical stacks showed diminished resolution around 150 μm in depth. We speculate that processes that increase epidermal thickness or disrupt epidermal architecture directly impair RCM evaluation of deeper structures. This is best exemplified by our decreased ability to detect detail in deeper layers of thick plaques and tumors. Second, our study was further limited by restricting our study sample to patients with confirmed MF/SS disease and therefore by having RCM and HP reviewers non-blinded to the diagnosis.

In conclusion, our study provides evidence for the clinical applicability of RCM in MF/SS. A major advantage of using RCM is the ability to noninvasively survey multiple skin lesions and large surface areas. Our data suggest that RCM examination may complement clinical, histopathologic and molecular examination for the diagnosis and management of MF/SS, and may improve patient outcomes, although we recognize the need for further studies to validate our findings.

References

1. Willemze R, Jaffe ES, Burg G, et al. WHO-EORTC classification for cutaneous lymphomas. Blood. 2005; 105:3768. [PubMed: 15692063]
2. Jaffe ES. The 2008 WHO classification of lymphomas: implications for clinical practice and translational research. Hematology Am Soc Hematol Educ Program. 2009; 523
3. Jawed SI, Myskowski PL, Horwitz S, Moskowitz A, Querfeld C. Primary cutaneous T-cell lymphoma (mycosis fungoides and Sezary syndrome): Part I. Diagnosis: clinical and histopathologic features and new molecular and biologic markers. J Am Acad Dermatol. 2014; 70:205.e1. [PubMed: 24438969]
4. Guitart J, Kennedy J, Ronan S, Chmiel JS, Hsiegh YC, Variakojis D. Histologic criteria for the diagnosis of mycosis fungoides: proposal for a grading system to standardize pathology reporting. J Cutan Pathol. 2001; 28:174. [PubMed: 11426824]
5. Agero AL, Gill M, Ardigo M, Myskowski P, Halpern AC, Gonzalez S. *In vivo* reflectance confocal microscopy of mycosis fungoides: a preliminary study. J Am Acad Dermatol. 2007; 57:435. [PubMed: 17433849]
6. Koller S, Gerger A, Ahlgrimm-Siess V, Weger W, Smolle J, Hofmann-Wellenhof R. *In vivo* reflectance confocal microscopy of erythematosquamous skin diseases. Exp Dermatol. 2009; 18:536. [PubMed: 19320740]
7. Lange-Asschenfeldt S, Babilli J, Beyer M, et al. Consistency and distribution of reflectance confocal microscopy features for diagnosis of cutaneous T cell lymphoma. J Biomed Opt. 2012; 17:016001. [PubMed: 22352651]
8. Li W, Dai H, Li Z, Xu AE. Reflectance confocal microscopy for the characterization of mycosis fungoides and correlation with histology: a pilot study. Skin Res Technol. 2013; 19:352. [PubMed: 23594100]
9. Ardigo M, El Shabrawi-Caelen L, Tosti A. *In vivo* reflectance confocal microscopy assessment of the therapeutic follow-up of cutaneous T-cell lymphomas causing scalp alopecia. Dermatol Ther. 2014; 27:248. [PubMed: 24754326]
10. Rajadhyaksha M, Gonzalez S, Zavislan JM, Anderson RR, Webb RH. *In vivo* confocal scanning laser microscopy of human skin II: advances in instrumentation and comparison with histology. J Invest Dermatol. 1999; 113:293. [PubMed: 10469324]

11. Rajadhyaksha M, Grossman M, Esterowitz D, Webb RH, Anderson RR. *In vivo* confocal scanning laser microscopy of human skin: melanin provides strong contrast. J Invest Dermatol. 1995; 104:946. [PubMed: 7769264]

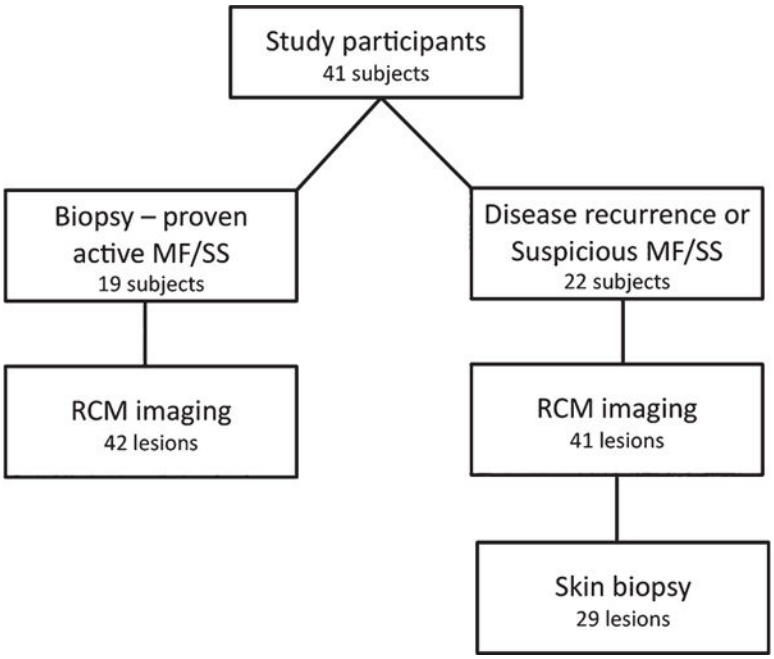

Fig. 1.

Study design and participants. Forty-one patients were included in the study. Nineteen participants were recently diagnosed mycosis fungoides/Sézary syndrome (MF/SS) patients with biopsy-proven active disease and 22 participants had suspicious MF/SS disease or disease recurrence. Among patients with suspicious MF/SS disease or disease recurrence, 29 biopsies were performed after reflectance confocal microscopy evaluation.

Fig. 2.

Clinical images of mycosis fungoides/Sézary syndrome lesions used for reflectance confocal microscopy. (A) Erythematous patch, (B) hypopigmented patch, (C) plaque, (D) hyperpigmented patches, (E) papules, (F) erythroderma, (G) diffuse erythroderma, (H) perifollicular papules and (I) poikiloderma.

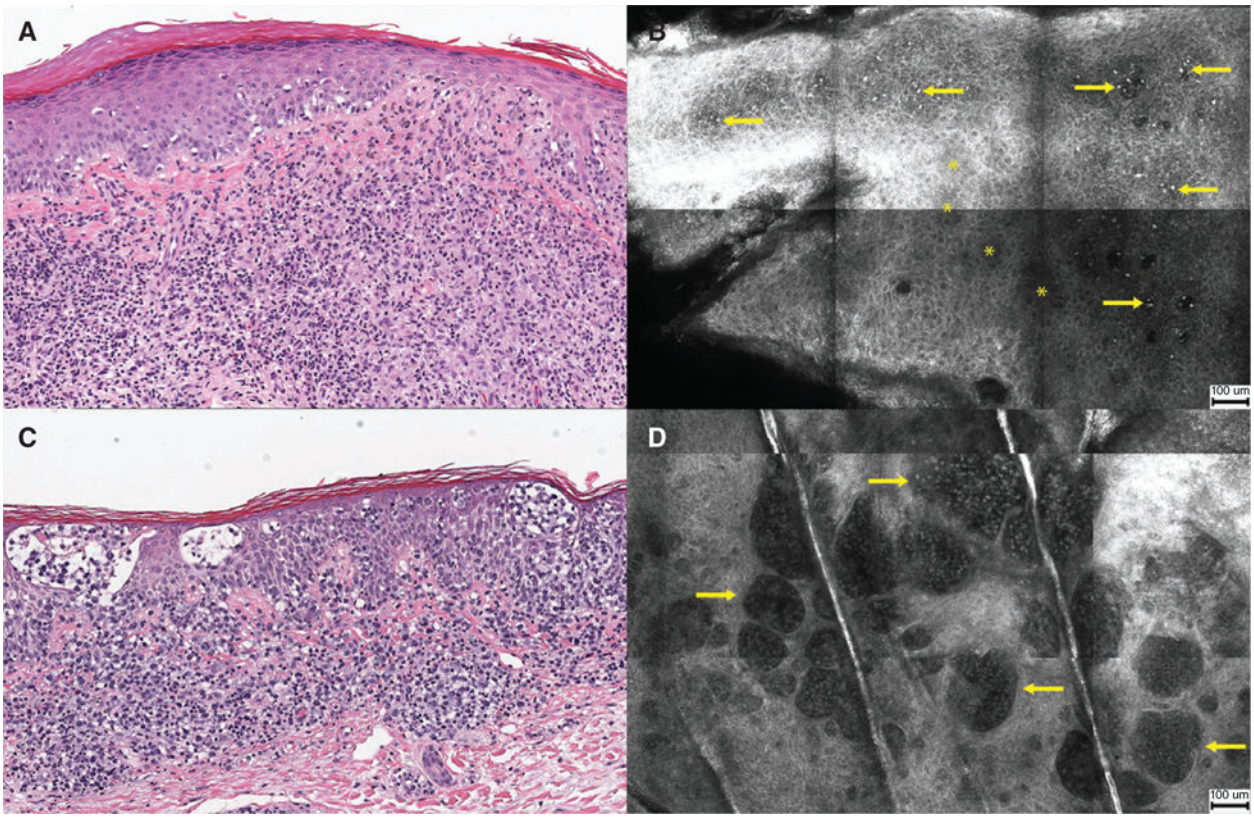

Fig. 3.

Histopathology and reflectance confocal microscopy (RCM) images of plaque lesions. (A) Atypical lymphocytes infiltrating the epidermis [hematoxylin & eosin (H&E) stain, original magnification ×100]. (B) RCM image showing brightly reflective cells (arrows) scattered in the stratum spinosum with focal areas of epidermal disarray (asterisk, *) (scale bar = 100 μm). (C) Collections of atypical lymphocytes forming Pautrier collections within epidermis (H&E, ×100). (D) RCM image showing well-demarcated, vesicle-like, dark spaces containing weakly reflective cells (arrows) (scale bar = 100 μm).

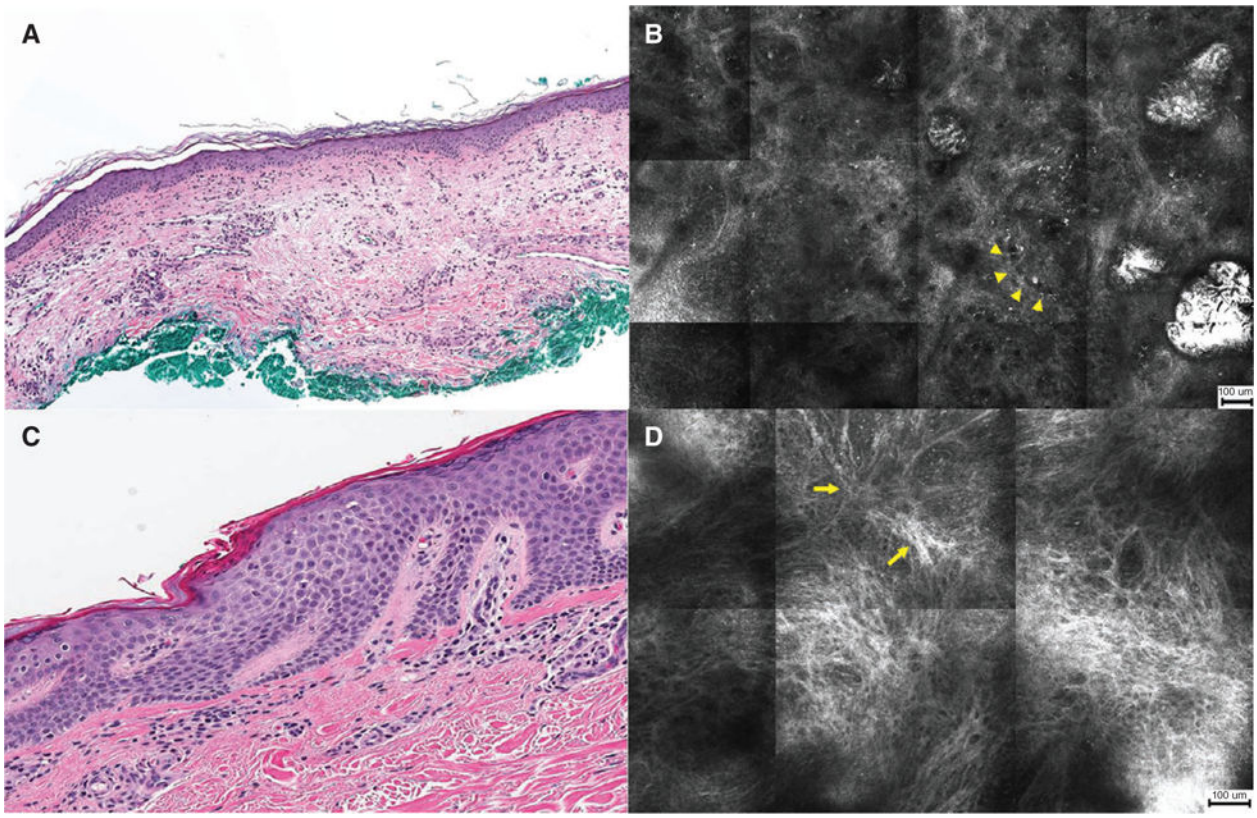

Fig. 4.

Histopathology and reflectance confocal microscopy (RCM) images of patch lesions. (A) Perivascular infiltration by atypical lymphocytes (H&E, ×50). (B) RCM image showing weakly reflective cells surrounding dilated canalicular structures in the papillary dermis (arrowheads) (scale bar = 100 μm). (C) HP showing fibrosis of upper papillary dermis (H&E, ×100). (D) RCM image showing disorganized distribution of reflective bundles (arrows) with scattered brightly reflective cells in the papillary dermis (scale bar = 100 μm).

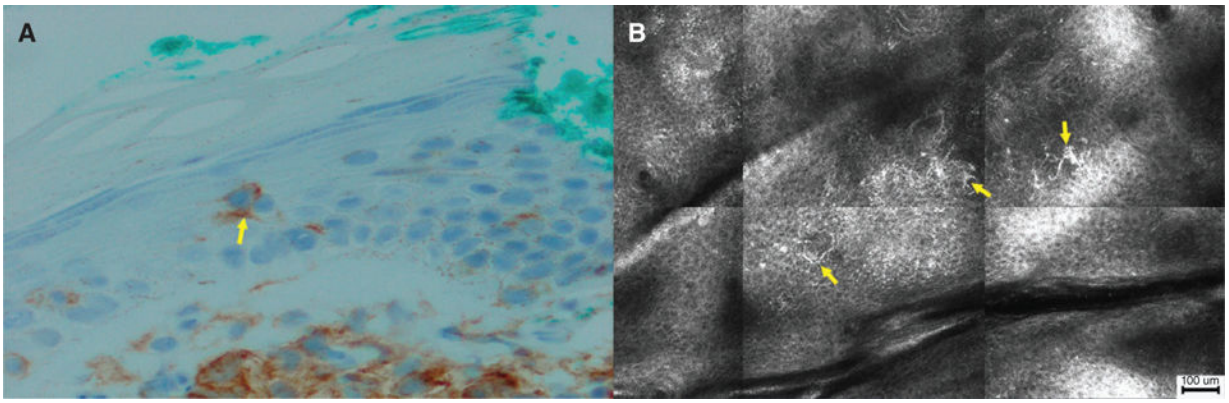

Fig. 5.

Histopathology and reflectance confocal microscopy (RCM) images of tumor lesions. (A) Langerhans cells in the epidermis (arrow) (CD4 immunohistochemical stain, ×200). (B) RCM image showing brightly reflective, dendritic cells with spinous processes (arrows) in the stratum spinosum (scale bar = 100 μm).

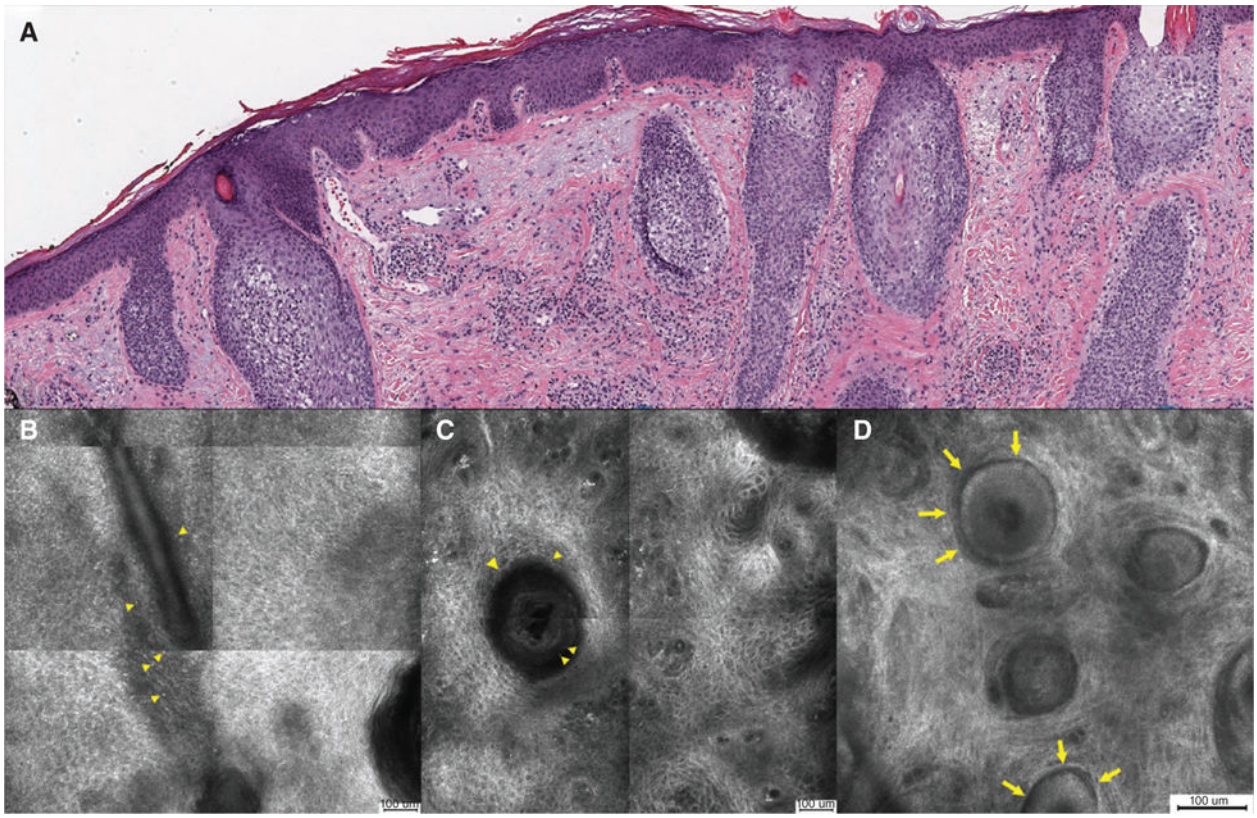

Fig. 6.

Histopathology and reflectance confocal microscopy (RCM) images of folliculotropic mycosis fungoides. (A) HP highlighting features of atypical lymphocytes surrounding and infiltrating hair follicles (H&E, ×50). (B) RCM image showing weakly reflective cells (arrowheads) surrounding and infiltrating follicular epithelium (scale bar = 100 μm). (C) RCM image showing weakly reflective cells (arrowheads) infiltrating follicular epithelium (scale bar = 100 μm). (D) RCM image showing mucinous deposition (arrows) appearing as hypo-reflective space surrounding follicular epithelium (scale bar = 100 μm).

Table 1

RCM parameters and morphologic descriptions

	RCM feature	Morphologic description
Epidermis		
1	Epidermal lymphocytes	Bright to weakly reflective cells with a round to oval cellular contour scattered throughout epidermal layers
2	Pautrier collections	Well-demarcated, vesicle-like, dark intraepidermal space containing scattered or clustered weakly reflective cells
3	Epidermal disarray/loss of demarcation	Loss of regular honeycomb pattern in the stratum spinosum. Epidermal layers showing lack of demarcation of individual keratinocytes and blurring of intercellular spaces. Patterns may be focal, multi-focal or diffuse
4	Spongiosis	Increased intercellular brightness with accentuation of keratinocyte borders
5	Dendritic cells	Bright epidermal cells with stellate morphology and dendritic processes
Dermal-epidermal junction		
6	DEJ lymphocytes	Weakly reflective cells with a round to oval cellular contour surrounding or infiltrating the basal layer
7	Hypo-reflective dermal rings	Decreased reflectivity of basal cells forming rings on the dermal papillae, compared to non-lesional skin
8	Hyper-reflective dermal rings	Increased reflectivity of basal cells forming rings on the dermal papillae, compared to non-lesional skin
Dermis		
9	Dermal lymphocytes	Weakly reflective cells with a round to oval cellular contour scattered within the papillary dermis or inside dermal papillae rings
10	Mixed infiltrate	Cells of varied reflectivity, size and morphology located in the papillary dermis or inside dermal papillae rings
11	Perivascular infiltrate	Weakly reflective cells with an irregular, round to oval cellular contour surrounding dilated canalicular structures in the papillary dermis
12	Blood vessel dilatation	Dilated, and often elongated, weakly reflective canalicular structures found at level of papillary dermis
13	Fibrosis	Disorganized distribution of bright reflective bundles in the papillary dermis
14	Melanophages	Large and bright reflective cells located in the papillary dermis or inside dermal papillae rings
Adnexal		
15	Follicular lymphocytes	Weakly reflective cells with an irregular, round to oval cellular contour surrounding or infiltrating follicular epithelium
16	Mucinous deposition	Hypo-reflective, amorphous space found within follicular epithelium

DEJ, dermoepidermal junction; RCM, reflectance confocal microscopy.

Table 2

Absolute and relative frequencies of RCM features of MF/SS skin lesions

		Lesion morphology							
	RCM features	**Erythematous patch (36); n (%)**	**Hyperpigmented patch (19); n (%)**	**Hypopigmented patch (1); n (%)**	**Papule (3); n (%)**	**Plaque (20); n (%)**	**Erythroderma (3); n (%)**	**Tumor (1); n (%)**	**Total (83); n (%)**
Epidermis	Epidermal lymphocytes	30 (83)	15 (79)	1 (100)	3 (100)	19 (95)	3 (100)	1 (100)	72 (86)
	Pautrier collections	15 (41)	8 (42)	0 (0)	2 (66)	16 (80)	2 (66)	1 (100)	44 (53)
	Epidermal disarray/loss of demarcation	30 (83)	16 (84)	1 (100)	3 (100)	19 (95)	3 (100)	1 (100)	73 (88)
	Dendritic processes	3 (8)	2 (10)	0 (0)	1 (33)	12 (60)	0 (0)	1 (100)	19 (23)
DEJ	DEJ lymphocytes	10 (27)	13 (68)	1 (100)	0 (0)	9 (45)	3 (100)	1 (100)	37 (44)
	Hypo-reflective dermal rings	35 (97)	1 (5)	1 (100)	2 (66)	18 (90)	3 (100)	1 (100)	60 (72)
	Hyper-reflective dermal rings	0 (0)	14 (73)	0 (0)	1 (33)	2 (10)	0 (0)	0 (0)	18 (21)
Dermis/adnexal	Dermal lymphocytes	6 (16)	7 (36)	0 (0)	1 (33)	5 (25)	3 (100)	1 (100)	23 (27)
	Follicular lymphocytes *	2 (5)	6 (31)	0 (0)	1 (33)	3 (15)	0 (0)	0 (0)	12 (14)
	Blood vessel dilation	32 (88)	10 (52)	1 (100)	2 (66)	17(85)	3 (100)	1 (100)	66 (79)
	Mixed infiltrate	11 (30)	12 (63)	0 (0)	2 (66)	5 (25)	1 (33)	1 (100)	32 (38)
	Perivascular infiltrate	6 (16)	4 (21)	0 (0)	0 (0)	2 (10)	1 (33)	1 (100)	14 (17)
	Fibrosis	13 (36)	1 (5)	0 (0)	2 (66)	7 (35)	1 (33)	1 (100)	25 (30)
	Melanophages	0 (0)	8 (42)	0 (0)	1 (33)	4 (20)	1 (33)	0 (0)	14 (17)

DEJ, dermal-epidermal junction; MF/SS, mycosis fungoides/Sézary syndrome; RCM, Reflectance confocal microscopy.

* One lesion showed concurrent adnexal mucinous deposition.

J Cutan Pathol. Author manuscript; available in PMC 2017 July 18.

Table 3

Correlation of RCM parameters with histopathologic features

	Incidence				
RCM and histopathology findings	**Histopathology; n (%)**	**RCM; n (%)**	**Agreement (%)**	**Kappa***	**p-value**
Epidermal lymphocytes	28 (97)	29 (100)	97	0.90†	
Melanophages in dermis	5 (17)	7 (24)	86	0.58	0.007
Pautrier collections	17 (59)	22 (76)	69	0.32	0.03
DEJ lymphocytes	23 (79)	20 (69)	62	0.24†	
Perivascular infiltrate	19 (66)	8 (28)	55	0.21	0.05
Dermal lymphocytes	4 (14)	11 (38)	61	0.16	0.14
Perifollicular infiltrate	3 (10)	5 (17)	79	0.14	0.21
Blood vessel dilation	18 (62)	26 (90)	66	0.15	0.14

DEJ, Dermal-epidermal junction; RCM, Reflectance confocal microscopy.

*Overall agreement is $\kappa = 0.41$, $p < 0.001$.

†Prevalence and bias-adjusted kappa (PABAK), p-value is not reported.